Chapter 7

Lasers

After having derived the quantum mechanically correct suszeptibility for an inverted atomic system that can provide gain, we can use the two-level model to study the laser and its dynamics. After discussing the laser concept briefly we will investigate various types of gain media, gas, liquid and solid-state, that can be used to construct lasers and amplifiers. Then the dynamics of lasers, threshold behavior, steady state behavior and relaxation oscillations are discussed. A short introduction in the generation of high energy and ultrashort laser pulses using Q-switching and mode locking will be given at the end.

7.1 The Laser (Oscillator) Concept

Since the invention of the vacuum amplifier tube by Robert von Lieben and Lee de Forest in 1905/06 it was known how to amplify electromagnetic waves over a broad wavelength range and how to build oscillator with which such waves could be generated. This was extended into the millimeter wave region with advances in amplifier tubes and later solid-state devices such as transistors. Until the 1950's thermal radiation sources were mostly used to generate electromagnetic waves in the optical frequency range. The generation of coherent optical waves was only made possible by the Laser. The first amplifier based on discrete energy levels (quantum amplifier) was the MASER (Microwave Amplification by Stimulated Emission of Radiation), which was invented by Gordon, Townes and Zeiger 1954. In 1958 Schawlow and Townes proposed to extend the MASER principle to the optical regime.

The amplification should arise from stimulated emission between discrete energy levels that must be inverted, as discussed in the last section. Amplifiers and oscillators based on this principle are called LASER (Light Amplification by Stimulated Emission of Radiation). Maiman was the first to demonstrate a laser based on the solid-state laser material Ruby.

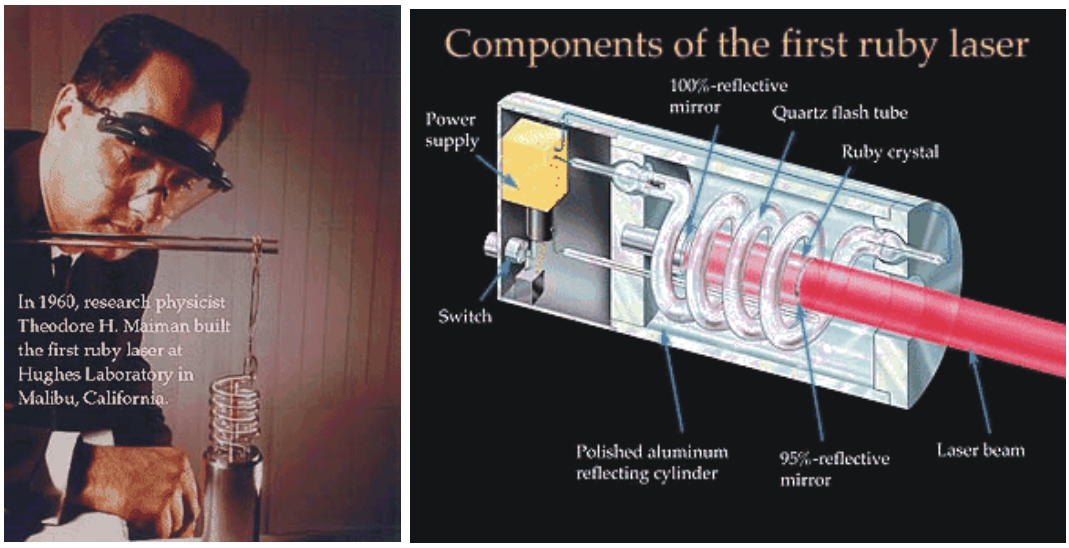

Figure 7.1: Theodore Maiman with the first Ruby Laser in 1960 and a cross sectional view of the first device [4].

The first HeNe-Laser, a gas laser followed in 1961. It is a gas laser built by Ali Javan at MIT, with a wavelength of 632.8 nm and a linewidth of only 10kHz.

The basic principle of an oscillator is a feedback circuit that is unstable, i.e. there is positive feedback at certain frequencies or certain frequency ranges, see Figure 7.2. It is the feedback circuit that determines the frequency of oscillation. Once the oscillation starts, the optical field will build up to an intensity approaching, or even surpassing, the saturation intensity of the amplifier medium by many times, until the amplifier gain is reduced to a value equal to the losses that the signal experiences after one roundtrip in the feedback loop, see Figure 7.3

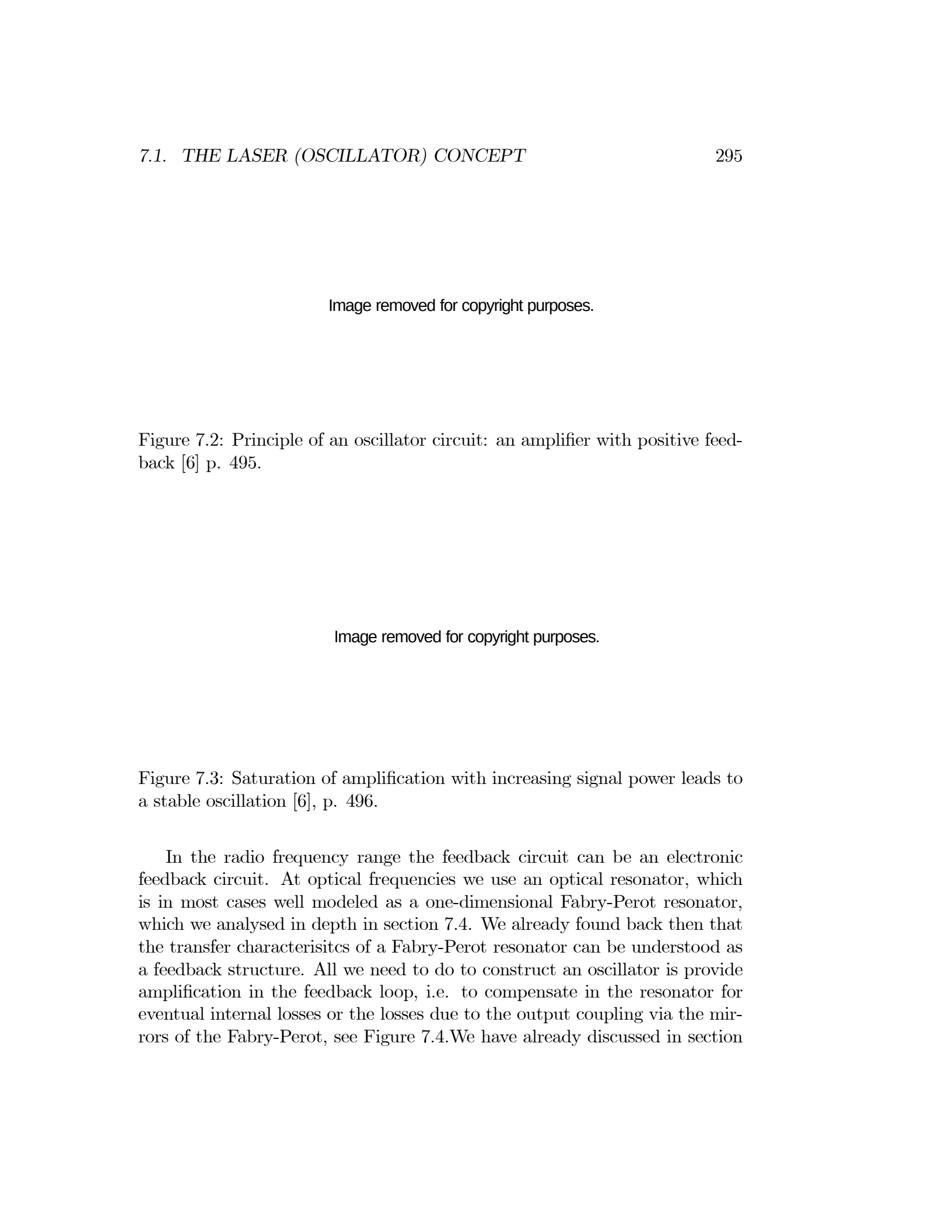

Figure 7.2: Principle of an oscillator circuit: an amplifier with positive feedback [6] p. 495.

Figure 7.3: Saturation of amplification with increasing signal power leads to a stable oscillation [6], p. 496.

In the radio frequency range the feedback circuit can be an electronic feedback circuit. At optical frequencies we use an optical resonator, which is in most cases well modeled as a one-dimensional Fabry-Perot resonator, which we analysed in depth in section 7.4. We already found back then that the transfer characterisitcs of a Fabry-Perot resonator can be understood as a feedback structure. All we need to do to construct an oscillator is provide amplification in the feedback loop, i.e. to compensate in the resonator for eventual internal losses or the losses due to the output coupling via the mirrors of the Fabry-Perot, see Figure 7.4.We have already discussed in section

2.6.2 various optical resonators, which have Gaussian beams as the fundamental resonator modes. One can also use waveguides or fibers that have semitransparent mirrors at its ends or form rings as laser resonators. In the latter ones output coupling of radiation is achieved with waveguide or fiber couplers in the rings.

Today lasers generating light continuosly or in the form of long, nanosecond, or very short, femtosecond pulses can be built. Typically these lasers are Q-switched or mode-locked, respectively. The average power level can vary from microwatt to kilowatts.

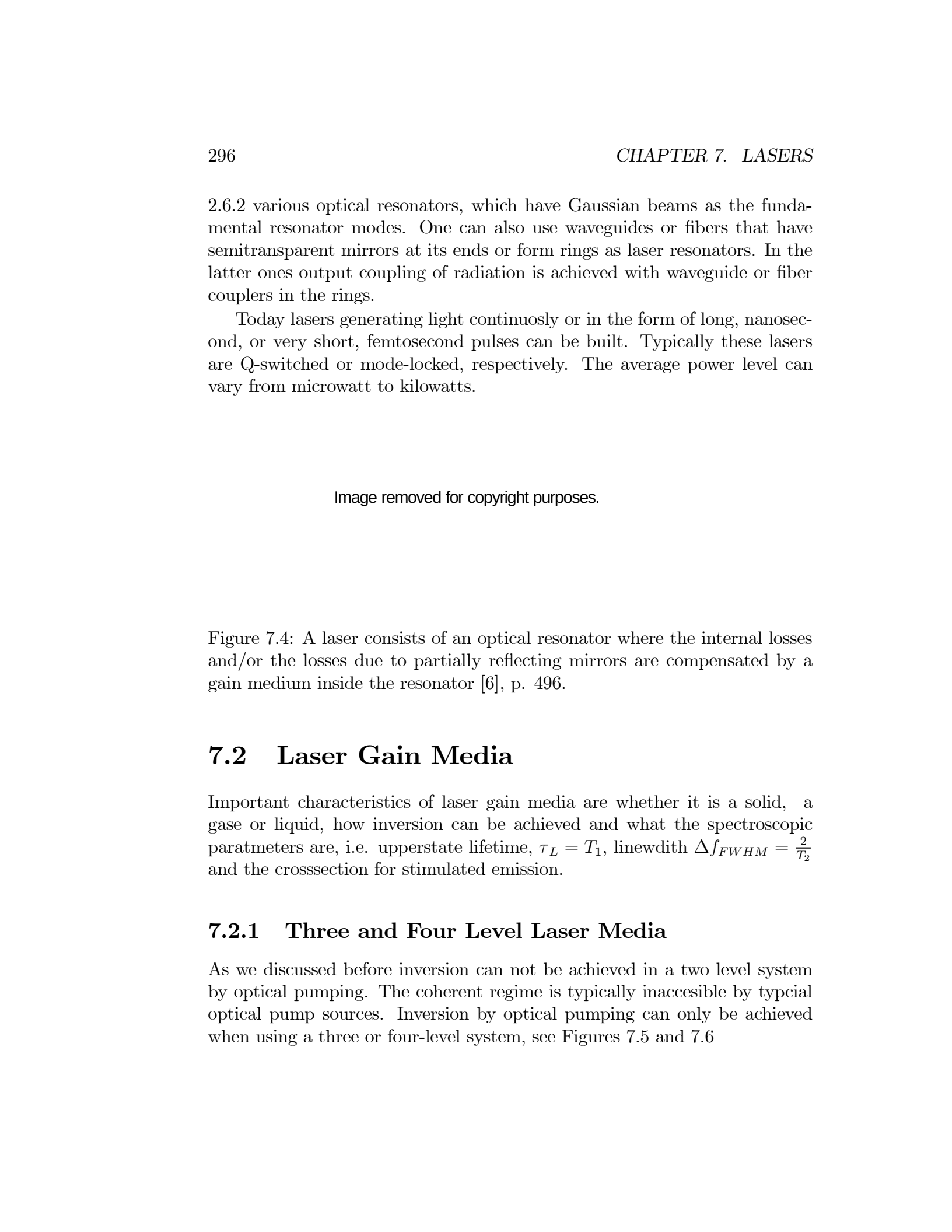

Figure 7.4: A laser consists of an optical resonator where the internal losses and/or the losses due to partially reflecting mirrors are compensated by a gain medium inside the resonator [6], p. 496.

7.2 Laser Gain Media

Important characteristics of laser gain media are whether it is a solid, a gase or liquid, how inversion can be achieved and what the spectroscopic paratmeters are, i.e. upperstate lifetime, $\tau_L = T_1$, linewdith $\Delta f_{FWHM} = \frac{2}{T_2}$ and the crosssection for stimulated emission.

7.2.1 Three and Four Level Laser Media

As we discussed before inversion can not be achieved in a two level system by optical pumping. The coherent regime is typically inaccesible by typcial optical pump sources. Inversion by optical pumping can only be achieved when using a three or four-level system, see Figures 7.5 and 7.6

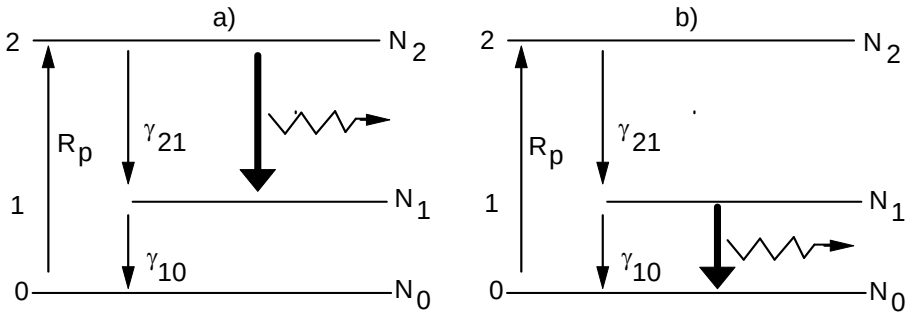

Figure 7.5: Three-level laser medium.

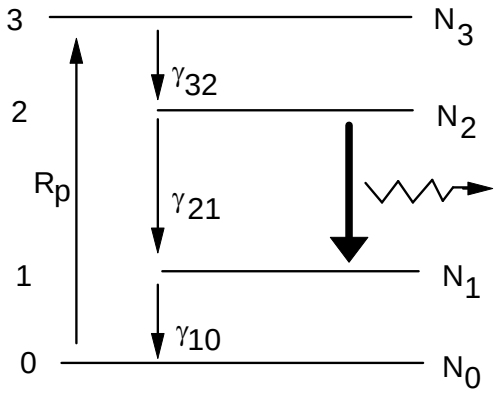

Figure 7.6: Four-level laser medium.

If the medium is in thermal equilibrium, typically only the ground state is occupied. By optical pumping with an intense lamp (flash lamp) or another laser one can pump a significant fraction of the atoms from the ground state with population N_0 into the excited state N_3 both for the three level laser operating according to scheme shown in figure 297 (a) or N_4 in the case

of the four level laser, see Figure 7.6. If the relaxation rate γ_{10} is very fast compared to γ_{21}, where the laser action should occur inversion can be achieved, i.e. $N_2 > N_1$. For the four level laser the relaxation rate γ_{32} should also be fast in comparison to γ_{21}. These systems are easy to analyze in the rate equation approximation, where the dipole moments are already adiabatically eliminated. For example, for the three level system in Figure 7.5 a). we obtain the rate equations of the three level system in analogy to the two-level system

$$\frac{d}{dt}N_2 = -\gamma_{21}N_2 - \sigma_{21}\left(N_2 - N_1\right)I_{ph} + R_p \tag{7.1}$$

$$\frac{d}{dt}N_1 = -\gamma_{10}N_1 + \gamma_{21}N_2 + \sigma_{21}\left(N_2 - N_1\right)I_{ph} \tag{7.2}$$

$$\frac{d}{dt}N_0 = \gamma_{10}N_1 - R_p \tag{7.3}$$

Here, σ_{21} is the cross section for stimulated emission between the levels 2 and 1 and I_{ph} is the photon flux at the transition frequency f_{21}.In most cases, there are any atoms available in the ground state such that optical pumping can never deplete the number of atoms in the ground state N_0. That is why we can assume a constant pump rate R_p. If the relaxation rate γ_{10} is much faster than γ_{21} and the number of possible stimulated emission events that can occur $\sigma_{21}\left(N_2 - N_1\right)I_{ph}$, then we can set $N_1 = 0$ and obtain only a rate equation for the upper laser level

$$\frac{d}{dt}N_2 = -\gamma_{21}\left(N_2 - \frac{R_p}{\gamma_{21}}\right) - \sigma_{21}N_2 \cdot I_{ph}. \tag{7.4}$$

This equation is identical to the equation for the inversion of the two-level system, see Eq.(6.125). Here, $\frac{R_p}{\gamma_{21}}$ is the equilibrium upper state population in the absence of photons, $\gamma_{21} = \frac{1}{\tau_L}$ is the inverse upper state lifetime due to radiative and non radiative processes.

Note, a similar analysis can be done for the three level laser operating according to the scheme shown in Figure 7.5 (b). Then the relaxation rate from level 3 to level 2, which is now the upper laser level has to be fast. But in addition the optical pumping must be so strong that essentially all the ground state levels are depleted. Undepleted groundstate populations would always lead to absorption of laser radiation.

In the following we want to discuss the electronic structure of a few often encountered laser media. A detail description of laser media can be found in [7].

7.3 Types of Lasers

7.3.1 Gas Lasers

Helium-Neon Laser

The HeNe-Laser is the most widely used noble gas laser. Lasing can be achieved at many wavelength 632.8nm (543.5nm, 593.9nm, 611.8nm, 1.1523μm, 1.52μm, 3.3913μm). Pumping is achieved by electrical discharge, see Figure 7.7.

Image removed for copyright purposes.

Figure 7.7: Energy level diagram of the transistions involved in the HeNe laser [9].

The helium is excited by electron impact. The energy is then transfered to Neon by collisions. The first HeNe laser operated at the 1.1523μm line [8]. HeNe lasers are used in many applications such as interferometry, holography, spectroscopy, barcode scanning, alignment and optical demonstrations.

Argon and Krypton Ion Lasers

Similar to the HeNe-laser the Argon ion gas laser is pumped by electric discharge and emitts light at wavelength: 488.0nm, 514.5nm, 351nm, 465.8nm, 472.7nm, 528.7nm.It is used in applications ranging from retinal phototherapy for diabetes, lithography, and pumping of other lasers.

The Krypton ion gas laser is analogous to the Argon gas laser with wavelength: 416nm, 530.9nm, 568.2nm, 647.1nm, 676.4nm, 752.5nm, 799.3nm. Pumped by electrical discharge. Applications range from scientific research. When mixed with argon it can be used as "white-light" lasers for light shows.

Carbon Lasers

In the carbon dioxide (CO_2) gas laser the laser transistions are related to vibrational-rotational excitations. CO_2 lasers are highly efficient approaching 30%. The main emission wavelengths are 10.6μm and 9.4μm. They are pumped by transverse (high power) or longitudinal (low power) electrical discharge. It is heavily used in the material processing industry for cutting, and welding of steel and in the medical area for surgery.

Carbon monoxide (CO) gas laser: Wavelength 2.6 - 4μm, 4.8 - 8.3μm pumped by electrical discharge. Also used in material processing such as engraving and welding and in photoacoustic spectroscopy. Output powers as high as 100kW have been demonstrated.

Excimer Lasers:

Chemical lasers emitting in the UV: 193nm (ArF), 248nm (KrF), 308nm (XeCl), 353nm (XeF) excimer (excited dimer). These are molecules that exist only if one of the atoms is electronically excited. Without excitation the two atoms repell each other. Thus the electronic groundstate is not stable and is therefore not populated, which is ideal for laser operation. These lasers are used for ultraviolet lithography in the semiconductor industry and laser surgery.

7.3.2 Dye Lasers:

The laser gain medium are organic dyes in solution of ethyl, methyl alcohol, glycerol or water. These dyes can be excited by optically with Argon lasers for example and emit at 390-435nm (stilbene), 460-515nm (coumarin 102),

570-640 nm (rhodamine 6G) and many others. These lasers have been widely used in research and spectroscopy because of there wide tuning ranges. Unfortunately, dyes are carcinogenic and as soon as tunable solid state laser media became available dye laser became extinct.

7.3.3 Solid-State Lasers

Ruby Laser

The first laser was indeed a solid-state laser: Ruby emitting at 694.3nm [5]. Ruby consists of the naturally formed crystal of aluminum oxide (Al_2O_3) called corundum. In that crystal some of Al^{3+} ions are replaced by Cr^{3+} ions. Its the chromium ions that give Ruby the pinkish color, i.e. its flourescence, which is related to the laser transisitons, see the level structure in Figure 7.8. Ruby is a three level laser.

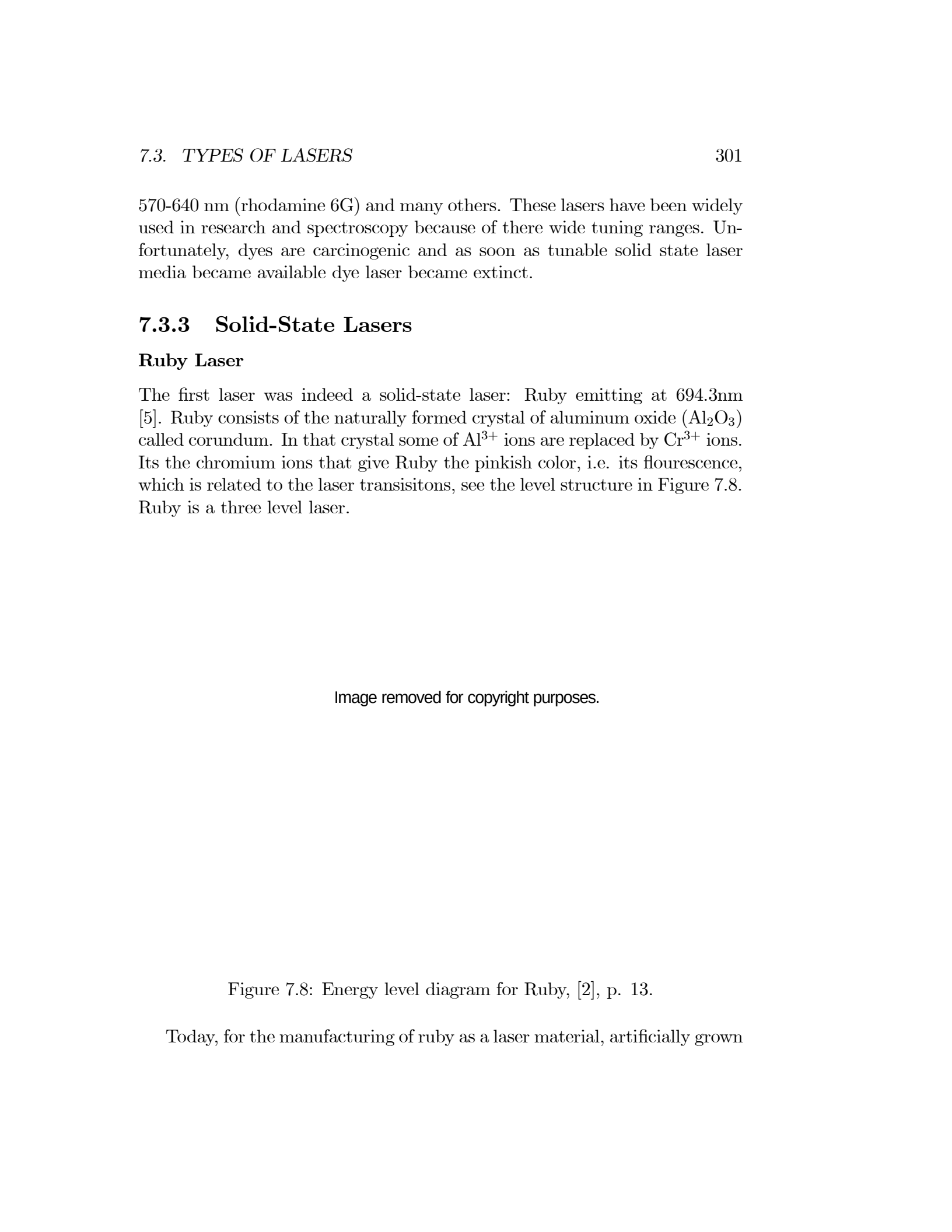

Figure 7.8: Energy level diagram for Ruby, [2], p. 13.

Today, for the manufacturing of ruby as a laser material, artificially grown

crystals from molten material which crystalizes in the form of sapphire is used. The liftetime of the upper laser level is 3ms. Pumping is usually achieved with flashlamps, see Figure 7.1.

Neodymium YAG (Nd:YAG)

Neodymium YAG consists of Yttrium-Aluminium-Garnet (YAG) $Y_3Al_5O_{12}$ in which some of the Y^{3+} ions are replaced by Nd^{3+} ions. Neodymium is a rare earth element, where the active electronic states are shielded inner $4f$ states. Nd:YAG is a four level laser, see Figure **??**.

Figure 7.9: Energy level diagram for Nd:YAG, [3], p. 370.

The main emission of Nd:YAG is at 1.064μm. Another line with considerable less gain is at 1.32μm. Initially Nd:YAG was flashlamp pumped. Today, much more efficient pumping is possible with laser diodes and diode arrays. Diode pumped versions which can be very compact and efficient become a competition for the CO_2 laser in material processing, range finding, surgery, pumping of other lasers in combination with frequency doubling to produce a green 532nm beam).

Neodymium can also be doped in a host of other crystals such as YLF (Nd:YLF) emitting at 1047μm, YVO4 (Nd:YVO) emitting at 1.064μm, glass (Nd:Glass) at 1.062μm (Silicate glasses), 1.054μm (Phosphate glasses). Glass lasers have been used to build extremely high power (Terawatt), high energy (Megajoules) multiple beam systems for inertial confinement fusion. The big advantage of glass is that it can be fabricated on meter scale which is hard or even impossible to do with crystalline materials.

Other rare earth elements are Er^{3+}, Tm^{3+}, Ho^{3+}, Er^{3+}, which have emmission lines at 1.53μm and in the 2-3μm range.

Ytterbium YAG (Yb:YAG)

Ytterbium YAG is a quasi three level laser, see Figure 303 emitting at 1.030μm. The lower laser level is only 500-600cm^{-1} (60meV) above the ground state and is therefore at room temperature heavily thermally populated. The laser is pumped at 941 or 968nm with laser diodes to provide the high brighness pumping needed to achieve gain.

Figure 7.10: Energy level diagram of Yb:YAG, [3], p. 374.

However, Yb:YAG has many advantages over other laser materials:

- Very low quantum defect, i.e. difference between the photon energy necessary for pumping and photon energy of the emitted radiation, $(hf_P - hf_L)/hf_P \tilde{} 9\%$.
- long radiative lifetime of the upper laser level, i.e. much energy can be stored in the crystal.
- high doping levels can be used without upper state lifetime quenching
- broad emission bandwidth of $\Delta f_{FWHM} = 2.5$THz enabling the generation of sub-picosecond pulses

- with cryogenic cooling Yb:YAG becomes a four level laser.

Due to the low quantum defect and the good thermal properties of YAG, Yb:YAG lasers approaching an optical to optical efficiency of 80% and a wall plug efficiency of 40% have been demonstrated.

Titanium Sapphire (Ti:sapphire)

In contrast to Neodymium, which is a rare earth element, Titanium is a transition metal. The Ti^{3+} ions replace a certain fraction of the Al^{3+} ions in sapphire (Al_2O_3). In transistion metal lasers, the laser active electronic states are outer 3s electrons which couple strongly to lattice vibrations. These lattice vibrations lead to strong line broadening. Therefore, Ti:sapphire has an extremely broad amplification linewidth $\Delta f_{FWHM} \approx 100$THz. Ti:sapphire can provide gain from 650-1080nm. Therefore, this material is used in todays highly-tunable or very short pulse laser systems and amplifiers. Once Ti:sapphire was developed it rapidly replaced the dye laser systems. Figure 7.11 shows the absorption and emission bands of Ti:sapphire for polarization along its optical axis ($\pi-$polarization).

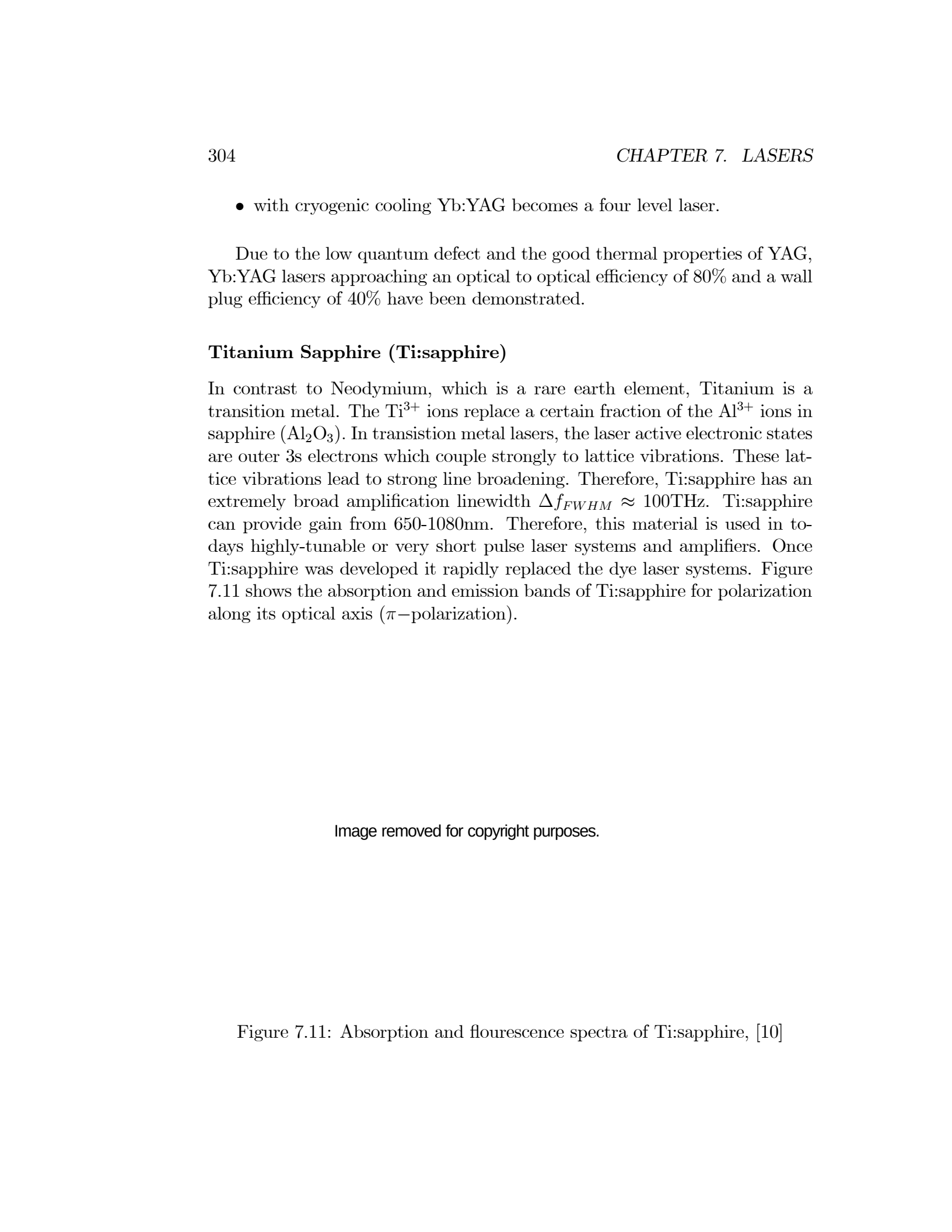

Figure 7.11: Absorption and flourescence spectra of Ti:sapphire, [10]

7.3.4 Semiconductor Lasers

An important class of solid-state lasers are semiconductor lasers. Depending on the semiconductor material used the emission wavelength can be further refined by using bandstructure engineering, 0.4 μm (GaN) or 0.63-1.55 μm (AlGaAs, InGaAs, InGaAsP) or 3-20 μm (lead salt). The AlGaAs based lasers in the wavelength range 670nm-780 nm are used in compact disc players and therefore are the most common and cheapest lasers in the world. In the semiconductor laser the electronic bandstructure is exploited, which arises from the periodic crystal potential, see problem set. The energy eigenstates can be characterized by the periodic crystal quasi momentum vector $\vec{k}$, see Figure

Figure 7.12: (a) Energy level diagram of the electronic states in a crystaline solid-state material. There is usually a highest occupied band, the valence band and a lowest unoccupied band the conduction band. Electronics states in a crystal can usually be characterized by their quasi momentum $\vec{k}$. b) The valence and conduction band are separated by a band gap.

Since the momentum carried along by an optical photon is very small compared to the momentum of the electrons in the crystal lattice, transistions of an electron from the valence band to the conduction band occur essentially vertically, see Figure 7.13 (a).

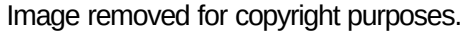

Figure 7.13: (a) At thermal equilibrium the valence band is occupied and the conduction band is unoccupied. Optical transistions occur vertically under momentum conservation, since the photon momentum is negligible compared to the momentum of the electrons. (b) To obtain amplification, the medium must be inverted, i.e. electrones must be accumulated in the conduction band and empty states in the valence band. The missing electron behave as a positively charged particles called holes.

Inversion, i.e. electrons in the conduction band and empty states in the valence band, holes, see Figure 7.13 (b) can be achieved by creating a pn-junction diode and forward biasing, see Figure 7.14.

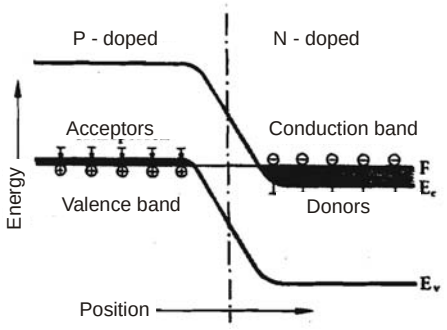

Figure 7.14: Forward biased pn-junction laser diode. Electrons and holes are injected into the space charge region of a pn-junction and emit light by recombination.

When forward-biased electrons and holes are injected into the space charge region. The carriers recombine and emit the released energy in the form of photons with an energy roughly equal to the band gap energy. A sketch of a typical pn-junction diode laser is shown in Figure 7.15.

Image removed for copyright purposes.

Figure 7.15: Typical broad area pn-homojunction laser, [3], p. 397.

The devices can be further refined by using heterojunctions so that the carriers are precisely confined to the region of the waveguide mode, see Figure

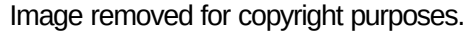

Figure 7.16: a) Refractive index profile. b) transverse beam profile, and c) band structure (shematic) of a double-heterostructure diode laser, [3], p. 399.

.

7.3.5 Quantum Cascade Lasers

A new form of semiconductor lasers was predicted in the 70's by the two russian physicists Kazarinov and Suris that is based only on one kind of electrical carriers. These are most often chosen to be electrons because of there higher mobility. This laser is therefore a unipolar device in contrast to the conventional semiconductor laser that uses both electrons and holes. the transitions are intraband transistions. A layout of a quantum cascade laser is shown in Figure 7.17.

Figure 7.17: Quantum Cascade laser layout.

Like semiconductor lasers these lasers are electrically pumped. The first laser of this type was realized in 1994 by Federico Capasso's group at Bell Laboratories [9], 23 years after the theoretical prediction. The reason for this is the difficult layer growth, that are only possible using advanced semiconductor growth capabilities such as molecular beam epitaxy (MBE) and more recently metal oxide chemical vapor depostion (MOCVD). Lasers have been demostrated in the few THz range [13] up to the 3.5μm region.

Some of the most important spectroscopic parameters of often used laser media are summarized in table 7.1.

7.3.6 Homogeneous and Inhomogeneous Broadening

Laser media are also distinguished by the line broadening mechanisms involved. Very often it is the case that the linewidth observed in the absorption or emission spectrum is not only due to dephasing process that are acting on

Laser Medium	Wave-length $\lambda_0(n\text{m})$	Cross Section σ (cm^2)	Upper-St. Lifetime τ_L (μs)	Linewidth $\Delta f_{FWHM} = \frac{2}{T_2}$(THz)	Typ	Refr. index n
Nd^{3+}:YAG	1,064	$4.1 \cdot 10^{-19}$	1,200	0.210	H	1.82
Nd^{3+}:LSB	1,062	$1.3 \cdot 10^{-19}$	87	1.2	H	1.47 (ne)
Nd^{3+}:YLF	1,047	$1.8 \cdot 10^{-19}$	450	0.390	H	1.82 (ne)
Nd^{3+}:YVO_4	1,064	$2.5 \cdot 10^{-19}$	50	0.300	H	2.19 (ne)
Nd^{3+}:glass	1,054	$4 \cdot 10^{-20}$	350	3	H/I	1.5
Er^{3+}:glass	1,55	$6 \cdot 10^{-21}$	10,000	4	H/I	1.46
Ruby	694.3	$2 \cdot 10^{-20}$	1,000	0.06	H	1.76
Ti^{3+}:Al_2O_3	660-1180	$3 \cdot 10^{-19}$	3	100	H	1.76
Cr^{3+}:LiSAF	760-960	$4.8 \cdot 10^{-20}$	67	80	H	1.4
Cr^{3+}:LiCAF	710-840	$1.3 \cdot 10^{-20}$	170	65	H	1.4
Cr^{3+}:LiSGAF	740-930	$3.3 \cdot 10^{-20}$	88	80	H	1.4
He-Ne	632.8	$1 \cdot 10^{-13}$	0.7	0.0015	I	$\sim$1
Ar^+	515	$3 \cdot 10^{-12}$	0.07	0.0035	I	$\sim$1
CO_2	10,600	$3 \cdot 10^{-18}$	2,900,000	0.000060	H	$\sim$1
Rhodamin-6G	560-640	$3 \cdot 10^{-16}$	0.0033	5	H	1.33
semiconductors	450-30,000	$\sim 10^{-14}$	~ 0.002	25	H/I	3 - 4

Table 7.1: Wavelength range, cross-section for stimulated emission, upper-state lifetime, linewidth, typ of lineshape (H=homogeneously broadened, I=inhomogeneously broadened) and index for some often used solid-state laser materials, and in comparison with semiconductor and dye lasers.

all atoms in the same, i.e. homogenous way. Lattice vibrations that lead to a line broadening of electronic transisitions of laser ions in the crystal act in the same way on all atoms in the crystal. Such mechanisms are called homogeneous broadening. However, It can be that in an atomic ensemble there are groups of atoms with a different center frequency of the atomic transistion. The overall ensemble therefore may eventually show a very broad linewidth but it is not related to actual dephasing mechanism that acts upon each atom in the ensemble. This is partially the case in Nd:silicate glass lasers, see table 7.1 and the linewidth is said to be inhomogeneously broadened. Wether a transistion is homogenously or inhomogeneously broadened can be tested by using a laser to saturate the medium. In a homogenously

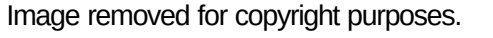

Figure 7.18: Laser with inhomogenously broaden laser medium (Nd:silicate glass) and homogenously broadened laser medium (Nd:phosphate glass), [14]

broadened medium the loss or gain saturates homogenously, i.e. the whole line is reduced. In an inhomogenously broadened medium a spectral hole burning occurs, i.e. only that sub-group of atoms that are sufficiently in resonance with the driving field saturate and the others not, which leads to a hole in the spectral distribution of the atoms. Figure 7.18 shows the impact of an inhomogeneously broadened gain medium on the continous wave output spectrum of a laser. In homogenous broadening leads to lasing of many longitudinal laser modes because inhomogenous saturation of the gain. In the homogenously broadened medium the gain saturates homogenously and only one or a few modes can lase. An important inhomogenous broadening mechanism in gases is doppler broadening. Due to the motion of the atoms in a gas relative to an incident electromagnetic beam, the center frequency of each atomic transistion is doppler shifted according to its velocity by

$$f = \left(1 \pm \frac{v}{c}\right) f_0, \tag{7.5}$$

where the plus sign is correct for an atom moving towards the beam and the minus sign for a atom moving with the beam. The velocity distribution of an ideal gas with atoms or molecules of mass m in thermal equilibrium is given by the Maxwell-Boltzman distribution

$$p(v) = \sqrt{\frac{m}{2\pi kT}} \exp\left(-\frac{mv^2}{2kT}\right). \tag{7.6}$$

This means that $p(v)dv$ is equal to the brobability that the atom or molecule has a velocity in the interval $[v, v + dv]$. Here, v is the component of the velocity that is in the direction of the beam. If the homogenous linewidth of the atoms is small compared to the doppler broading, we obtain the lineshape of the inhomogenously broadened gas simply by substituting the velocity by the induced frequency shift due to the motion

$$v = c\,\frac{f - f_0}{f_0} \tag{7.7}$$

Then the lineshape is a Gaussian

$$g(f) = \sqrt{\frac{mc}{2\pi kT f_0}}\exp\left[-\frac{mc^2}{2kT}\left(\frac{f - f_0}{f_0}\right)^2\right]. \tag{7.8}$$

The full width at half maximum of the line is

$$\Delta f = 8\ln(2)\sqrt{\frac{kT}{mc^2}}f_0. \tag{7.9}$$

7.4 Laser Dynamics (Single Mode)

In this section we want study the single mode laser dynamics. The laser typically starts to lase in a few closely spaced longitudinal modes, which are incoherent with each other and the dynamics is to a large extent similar to the dynamics of a single mode that carries the power of all lasing modes. To do so, we complement the rate equations for the populations in the atomic medium, that can be reduced to the population of the upper laser level Eq.(7.4) as discussed before with a rate equation for the photon population in the laser mode.

There are two different kinds of laser cavities, linear and ring cavities, see Figure 7.19

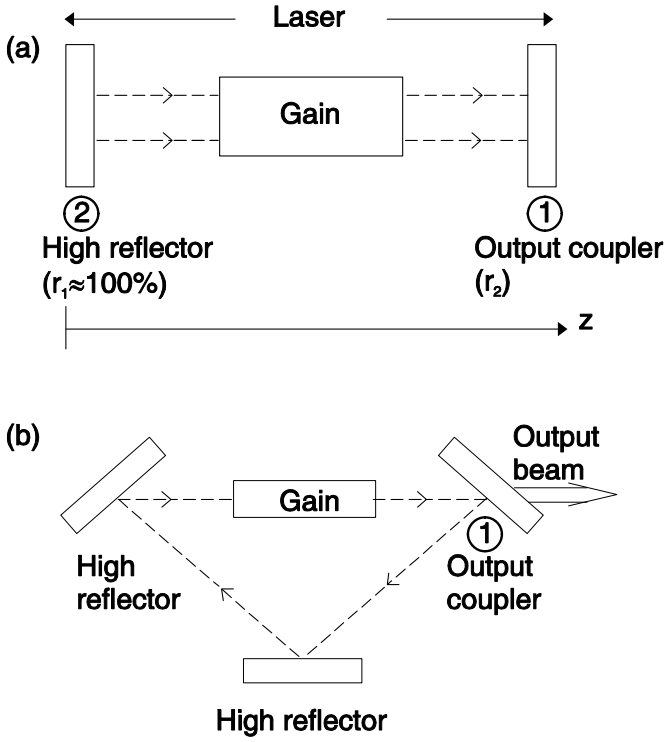

Figure 7.19: Possible cavity configurations. (a) Schematic of a linear cavity laser. (b) Schematic of a ring laser.

The laser resonators can be modelled as Fabry Perots as discussed in section . Typically the techniques are used to avoid lasing of transverse modes and only the longitudinal modes are of interest. The resonance frequencies of the longitudinal modes are determined by the round trip phase to be a multiple of 2π

$$\phi(\omega_m) = 2m\pi. \tag{7.10}$$

neighboring modes are space in frequency by the inverse roundtrip time

$$\phi(\omega_0 + \Delta\omega) = \phi(\omega_0) + T_R\Delta\omega = 2m\pi. \tag{7.11}$$

T_R is the round trip time in the resonator, which is

$$T_R = \frac{2^* L}{\nu_g}, \tag{7.12}$$

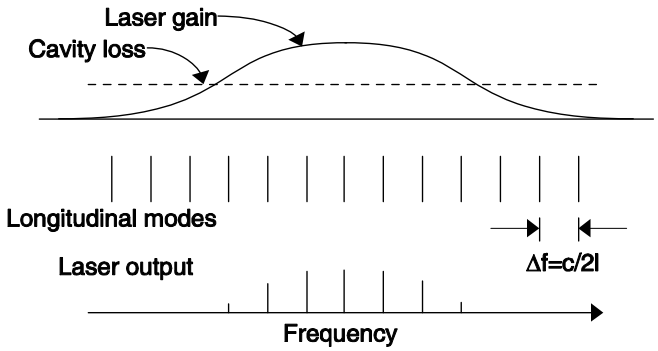

Figure 7.20: Laser gain and cavity loss spectra, longitudinal mode location, and laser output for multimode laser operation.

where ν_g is the group velocity in the cavity in the frequency range considered, and L is the cavity length of the linear or ring cavity and $2^* = 1$ for the ring cavity and $2^* = 2$ for the linear cavity. In the case of no dispersion, the longitudinal modes of the resonator are multiples of the inverse roundtrip timeand

$$f_m = m\frac{1}{T_R}. \tag{7.13}$$

The mode spacing of the longitudinal modes is

$$\Delta f = f_m - f_{m-1} = \frac{1}{T_R} \tag{7.14}$$

If we assume frequency independent cavity loss and Lorentzian shaped gain (see Fig. 7.20). Initially when the laser gain is larger then the cavity loss, many modes will start to lase. To assure single frequency operation a filter (etalon) can be inserted into the laser resonator, see Figure 7.21. If the laser is homogenously broadened the laser gain will satured to the loss level and only the mode at the maximum of the gain will lase. If the gain is not homogenously broadend and in the absence of a filter many modes will lase.

For the following we assume a homogenously broadend laser medium and only one cavity mode is able to lase. We want to derive the equations of motion for th population inversion, or population in the upper laser level and the photon number in that mode, see Figure 7.22.

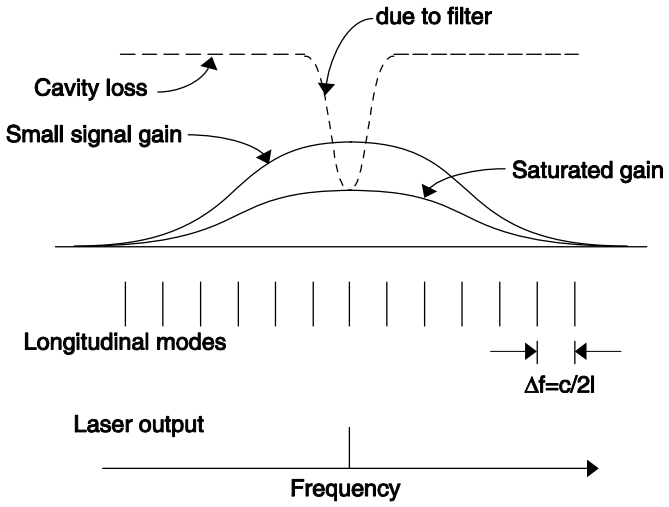

Figure 7.21: Gain and loss spectra, longitudinal mode locations, and laser output for single mode laser operation.

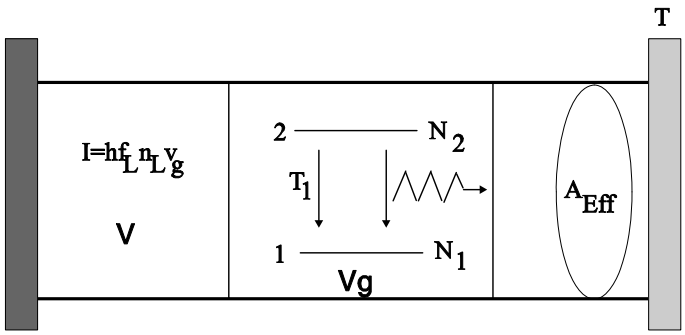

Figure 7.22: Rate equations for a laser with two-level atoms and a resonator.

The intensity I in a mode propagating at group velocity v_g with a mode volume V is related to the number of photons N_L or the number density $n_L = N_L/V$ stored in the mode with volume V by

$$I = hf_L \frac{N_L}{2^* V} v_g = \frac{1}{2^*} hf_L n_L v_g, \tag{7.15}$$

where hf_L is the photon energy. $2^* = 2$ for a linear laser resonator (then only half of the photons are going in one direction), and $2^* = 1$ for a ring

laser. In this first treatment we consider the case of space-independent rate equations, i.e. we assume that the laser is oscillating on a single mode and pumping and mode energy densities are uniform within the laser material. With the interaction cross section σ for stimulated emission defined as

$$\sigma = \frac{hf_L}{I_s T_1}, \tag{7.16}$$

and Eq. (7.4) with the number of atoms in the mode, we obtain

$$\frac{d}{dt}N_2 = -\frac{N_2}{\tau_L} - 2^*\sigma N_2 v_g n_L + R_p. \tag{7.17}$$

Here, $v_g n_L$ is the photon flux, σ is the stimulated emission cross section, $\tau_L = \gamma_{21}$ the upper state lifetime and R_p is the pumping rate into the upper laser level. A similar rate equation can be derived for the photon density

$$\frac{d}{dt}n_L = -\frac{n_L}{\tau_p} + 2^*\frac{\sigma v_g}{V}N_2\left(n_L + \frac{1}{V}\right). \tag{7.18}$$

Here, τ_p is the photon lifetime in the cavity or cavity decay time. The $1/V$ -term in Eq.(7.18) accounts for spontaneous emission which is equivalent to stimulated emission by one photon occupying the mode with mode volume V. For a laser cavity with a semi-transparent mirror with amplitude transmission T, see section 2.3.8, producing a power loss $2l = 2T$ per round-trip in the cavity, the cavity decay time is $\tau_p = 2l/T_R$, if $T_R = 2^*L/c_0$ is the roundtrip-time in linear cavity with optical length $2L$ or a ring cavity with optical length L. Eventual internal losses can be treated in a similar way and contribute to the cavity decay time. Note, the decay rate for the inversion in the absence of a field, $1/\tau_L$, is not only due to spontaneous emission, but is also a result of non radiative decay processes. See for example the four level system shown in Fig. 7.6.

So the two rate equations are

$$\frac{d}{dt}N_2 = -\frac{N_2}{\tau_L} - 2^*\sigma v_g N_2 n_L + R_p \tag{7.19}$$

$$\frac{d}{dt}n_L = -\frac{n_L}{\tau_p} + 2^*\frac{\sigma v_g}{V}N_2\left(n_L + \frac{1}{V}\right). \tag{7.20}$$

Experimentally, the photon number and the inversion in a laser resonator are not very convenient quantities, therefore, we normalize both equations to

the round-trip amplitude gain $g = 2^* \frac{\sigma v_g}{2V} N_2 T_R$ experienced by the light and the circulating intracavity power $P = I \cdot A_{eff}$

$$\frac{d}{dt}g = -\frac{g - g_0}{\tau_L} - \frac{gP}{E_{sat}} \tag{7.21}$$

$$\frac{d}{dt}P = -\frac{1}{\tau_p}P + \frac{2g}{T_R}\left(P + P_{vac}\right), \tag{7.22}$$

with

$$E_{sat} = \frac{hf_L}{2^*\sigma}A_{eff} = \frac{1}{2^*}I_s A_{eff}\tau_L \tag{7.23}$$

$$P_{sat} = E_s/\tau_L \tag{7.24}$$

$$P_{vac} = hf_L v_g/2^* L = hf_L/T_R \tag{7.25}$$

$$g_0 = 2^* \frac{R_p}{2A_{eff}}\sigma\tau_L, \tag{7.26}$$

the small signal round-trip gain of the laser. Note, the factor of two in front of gain and loss is due to the fact, that we defined g and l as gain and loss with respect to amplitude. Eq.(7.26) elucidates that the figure of merit that characterizes the small signal gain achievable with a certain laser material is the $\sigma\tau_L$-product.

7.5 Continuous Wave Operation

If $P_{vac} \ll P \ll P_{sat} = E_{sat}/\tau_L$, than $g = g_0$ and we obtain from Eq.(7.22), neglecting P_{vac}

$$\frac{dP}{P} = 2\left(g_0 - l\right)\frac{dt}{T_R} \tag{7.27}$$

or

$$P(t) = P(0)e^{2(g_0 - l)\frac{t}{T_R}}. \tag{7.28}$$

The laser power builts up from vaccum fluctuations, see Figure 7.23 until it reaches the saturation power, when saturation of the gain sets in within the built-up time

$$T_B = \frac{T_R}{2\left(g_0 - l\right)}\ln\frac{P_{sat}}{P_{vac}} = \frac{T_R}{2\left(g_0 - l\right)}\ln\frac{A_{eff}T_R}{\sigma\tau_L}. \tag{7.29}$$

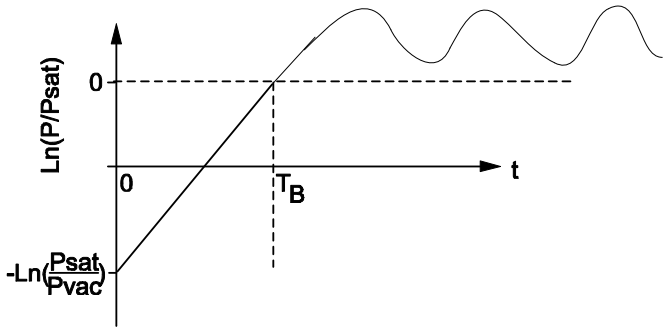

Figure 7.23: Built-up of laser power from spontaneous emission noise.

Some time after the built-up phase the laser reaches steady state, with the saturated gain and steady state power resulting from Eqs.(7.21-7.22), neglecting in the following the spontaneous emission, $P_{vac} = 0$, and for $\frac{d}{dt} = 0$:

$$g_s = \frac{g_0}{1 + \frac{P_s}{P_{sat}}} = l \tag{7.30}$$

$$P_s = P_{sat}\left(\frac{g_0}{l} - 1\right), \tag{7.31}$$

Figure 7.24 shows output power and gain as a function of small signal gain g_0, which is proportional to the pump rate. Below threshold, the output power is zero and the gain increases linearly with in crease pumping. After reaching threshold the gain stays clamped at the threshold value determined by gain equal loss and the output power increases linearly.

7.6 Stability and Relaxation Oscillations

How does the laser reach steady state, once a perturbation has occured?

$$g = g_s + \Delta g \tag{7.32}$$

$$P = P_s + \Delta P \tag{7.33}$$

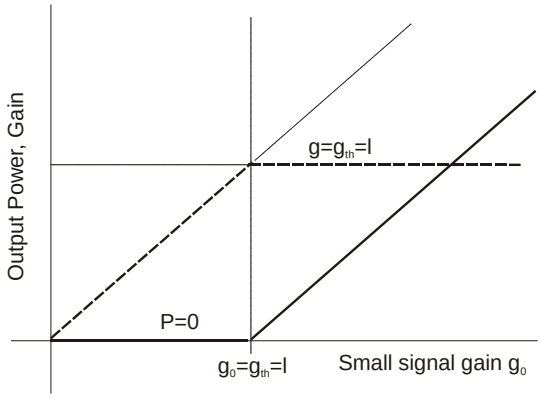

Figure 7.24: Output power and gain of a laser as a function of pump power.

Substitution into Eqs.(7.21-7.22) and linearization leads to

$$\frac{d\Delta P}{dt} = +2\frac{P_s}{T_R}\Delta g \tag{7.34}$$

$$\frac{d\Delta g}{dt} = -\frac{g_s}{E_{sat}}\Delta P - \frac{1}{\tau_{stim}}\Delta g \tag{7.35}$$

where $\frac{1}{\tau_{stim}} = \frac{1}{\tau_L}\left(1 + \frac{P_s}{Psat}\right)$ is the inverse stimulated lifetime. The stimulated lifetime is the lifetime of the upper laser state in the presence of the optical field. The perturbations decay or grow like

$$\begin{pmatrix} \Delta P \\ \Delta g \end{pmatrix} = \begin{pmatrix} \Delta P_0 \\ \Delta g_0 \end{pmatrix} e^{st}. \tag{7.36}$$

which leads to the system of equations (using $g_s = l$)

$$A \begin{pmatrix} \Delta P_0 \\ \Delta g_0 \end{pmatrix} = \begin{pmatrix} -s & 2\frac{P_s}{T_R} \\ -\frac{T_R}{E_{sat}2\tau_p} & -\frac{1}{\tau_{stim}} - s \end{pmatrix} \begin{pmatrix} \Delta P_0 \\ \Delta g_0 \end{pmatrix} = 0. \tag{7.37}$$

There is only a solution, if the determinante of the coefficient matrix vanishes, i.e.

$$s\left(\frac{1}{\tau_{stim}} + s\right) + \frac{P_s}{E_{sat}\tau_p} = 0, \tag{7.38}$$

which determines the relaxation rates or eigen frequencies of the linearized system

$$s_{1/2} = -\frac{1}{2\tau_{stim}} \pm \sqrt{\left(\frac{1}{2\tau_{stim}}\right)^2 - \frac{P_s}{E_{sat}\tau_p}}. \tag{7.39}$$

Introducing the pump parameter $r = 1 + \frac{P_s}{P_{sat}}$, which tells us how often we pump the laser over threshold, the eigen frequencies can be rewritten as

$$s_{1/2} = -\frac{1}{2\tau_{stim}} \left(1 \pm j \sqrt{\frac{4\,(r-1)}{r} \frac{\tau_{stim}}{\tau_p} - 1} \right), \tag{7.40}$$

$$= -\frac{r}{2\tau_L} \pm j \sqrt{\frac{(r-1)}{\tau_L \tau_p} - \left(\frac{r}{2\tau_L} \right)^2} \tag{7.41}$$

There are several conclusions to draw:

- (i): The stationary state $(0, g_0)$ for $g_0 < l$ and (P_s, g_s) for $g_0 > l$ are always stable, i.e. $\mathrm{Re}\{s_i\} < 0$.
- (ii): For lasers pumped above threshold, $r > 1$, and long upper state lifetimes, i.e. $\frac{r}{4\tau_L} < \frac{1}{\tau_p}$,

  the relaxation rate becomes complex, i.e. there are relaxation oscillations

  $$s_{1/2} = -\frac{1}{2\tau_{stim}} \pm j\omega_R. \tag{7.42}$$

  with a frequency ω_R approximately equal to the geometric mean of inverse stimulated lifetime and photon life time

  $$\omega_R \approx \sqrt{\frac{1}{\tau_{stim}\tau_p}}. \tag{7.43}$$

- If the laser can be pumped strong enough, i.e. r can be made large enough so that the stimulated lifetime becomes as short as the cavity decay time, relaxation oscillations vanish.

The physical reason for relaxation oscillations and instabilities related to it is, that the gain reacts to slow on the light field, i.e. the stimulated lifetime is long in comparison with the cavity decay time.

Example: diode-pumped Nd:YAG-Laser

$$\begin{aligned} \lambda_0 &= 1064 \text{ nm}, \sigma = 4 \cdot 10^{-20} cm^2,\ A_{eff} = \pi\,(100\mu m \times 150\mu m)\,, r = 50 \\ \tau_L &= 1.2\ ms,\ l = 1\%,\ T_R = 10ns \end{aligned}$$

From Eq.(7.16) we obtain:

$$\begin{aligned} I_{sat} &= \frac{hf_L}{\sigma\tau_L} = 3.9\frac{kW}{cm^2},\ P_{sat} = I_{sat}A_{eff} = 1.8\ W,\ P_s = 91.5W \\ \tau_{stim} &= \frac{\tau_L}{r} = 24\mu s,\ \tau_p = 1\mu s, \omega_R = \sqrt{\frac{1}{\tau_{stim}\tau_p}} = 2\cdot 10^5 s^{-1}. \end{aligned}$$

Figure 7.25 shows the typically observed fluctuations of the output of a solid-

Figure 7.25: Relaxation oscillations in the time and frequency domain.

state laser in the time and frequency domain. Note, that this laser has a long upperstate lifetime of several 100 μs

One can also define a quality factor for the relaxation oscillations by the ratio of the imaginary to the real part of the complex eigen frequencies 7.41

$$Q = \sqrt{\frac{4\tau_L}{\tau_p}\frac{(r-1)}{r^2}}. \tag{7.44}$$

The quality factor can be as large a several thousand for solid-state lasers with long upper-state lifetimes in the millisecond range.

7.7 Laser Efficiency

An important measure for a laser is the efficiency with which pump power is converted into laser output power. To determine the efficiency we must review the important parameters of a laser and the limitations these parameters impose.

From Eq.(7.31) we found that the steady state intracavity power P_s of a laser is

$$P_s = P_{sat}\left(\frac{2g_0}{2l} - 1\right), \tag{7.45}$$

where $2g_0$ is the small signal round-trip power gain, P_{sat} the gain saturation power and $2l$ is the power loss per round-trip. Both parameters are expressed in terms of the fundamental pump parameter R_p, $\sigma\tau_L$-product and mode cross section A_{eff} of the gain medium. For this derivation it was asummed that all pumped atoms are in the laser mode with constant intensity over the beam cross section

$$2g_0 = 2^* \frac{R_p}{A_{eff}}\sigma\tau_L, \tag{7.46}$$

$$P_{sat} = \frac{hf_L}{2^*\sigma\tau_L}A_{eff} \tag{7.47}$$

The power losses of lasers are due to the internal losses $2l_{int}$ and the transmission T through the output coupling mirror. The internal losses can be a significant fraction of the total losses. The output power of the laser is

$$P_{out} = T \cdot P_{sat}\left(\frac{2g_0}{2l_{int} + T} - 1\right) \tag{7.48}$$

The pump power of a laser is minimized given

$$P_p = R_p h f_P, \tag{7.49}$$

where hf_P is the energy of the pump photons. In discussing the efficiency of a laser, we consider the overall efficiency

$$\eta = \frac{P_{out}}{P_p} \tag{7.50}$$

which approaches the differential efficiency η_D if the laser is pumped many times over threshold, i.e. $r = 2g_0/2l \to \infty$

$$\eta_D = \frac{\partial P_{out}}{\partial P_p} = \eta(r \to \infty) \tag{7.51}$$

$$= \frac{T}{2l_{int} + T} P_{sat} \frac{2^*}{A_{eff} h f_P} \sigma \tau_L \tag{7.52}$$

$$= \frac{T}{2l_{int} + T} \cdot \frac{h f_L}{h f_P}. \tag{7.53}$$

Thus the efficiency of a laser is fundamentally limited by the ratio of output coupling to total losses and the quantum defect in pumping. Therefore, one would expect that the optimum output coupling is achieved with the largest output coupler, however, this is not true as we considered the case of operating many times above threshold.

7.8 "Thresholdless" Lasing

So far we neglected the spontaneous emission into the laser mode. This is justified for large lasers where the density of radiation modes in the laser medium is essentially the free space mode density and effects very close to threshold are not of interest. For lasers with small mode volume, or a laser operating very close to threshold, the spontaneous emission into the laser mode can no longer be neglected and we should use the full rate equations (7.21) and (7.22)

$$\frac{d}{dt} g = -\frac{g - g_0}{\tau_L} - \frac{gP}{E_{sat}} \tag{7.54}$$

$$\frac{d}{dt} P = -\frac{1}{\tau_p} P + \frac{2g}{T_R} \left(P + P_{vac} \right), \tag{7.55}$$

where P_{vac} is the power of a single photon in the mode. The steady state conditions are

$$g_s = \frac{g_0}{(1 + P_s/P_{sat})}, \tag{7.56}$$

$$0 = \left(2g_s - 2l \right) P + 2 g_s P_{vac}. \tag{7.57}$$

Substitution of the saturated gain condition (7.56) into (7.57) and using the pump parameter $r = 2g_0/2l$, leads to a quadratic equation for the normalized intracavity steady state power $p{=}P_s/P_{sat}$ in terms of normalized vacuum power $p_v = P_{vac}/P_{sat} = \sigma\tau_L v_g/V$. This equation has the solutions

$$p = \frac{r-1+rp_v}{2} \pm \sqrt{\left(\frac{r-1+rp_v}{2}\right)^2 + (rp_v)^2}. \tag{7.58}$$

where only the solution with the plus sign is of physical significance. Note, the typical value for the $\sigma\tau_L$-product of the laser materials in table 7.1 is $\sigma\tau_L = 10^{-23} cm^2 s$. If the volume is measured in units of wavelength cubed we obtain $p_v = 0.3/\beta$ for$\lambda = 1\mu m, V = \beta\lambda^3$ and $v_g = c$. Figure 7.26 shows the behavior of the intracavity power as a function of the pump parameter for various values of the normalized vacuum power.

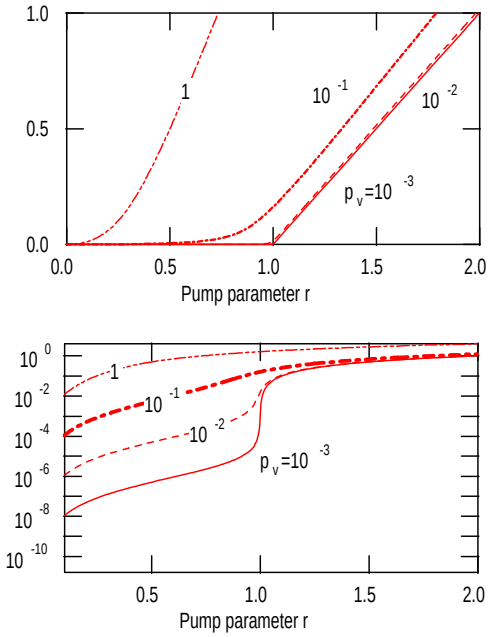

Figure 7.26: Intracavity power as a function of pump parameter r on a linear scale (a) and a logarithmic scale (b) for various values of the normalized vacuum power.

Figure 7.26 shows that for lasers with small mode volumes, i.e. mode volumes of the size of the wavelength cubed, the threshold is no longer well defined.

7.9 Short pulse generation by Q-Switching

The energy stored in the laser medium can be released suddenly by increasing the Q-value of the cavity so that the laser reaches threshold. This can be done actively, for example by quickly moving one of the resonator mirrors in place or passively by placing a saturable absorber in the resonator [**?**, 8]. Hellwarth first suggest this method only one year after the invention of the laser. As a rough orientation for a solid-state laser the following relation for the relevant time scales is generally valid

$$\tau_L \gg T_R \gg \tau_p. \tag{7.59}$$

7.9.1 Active Q-Switching

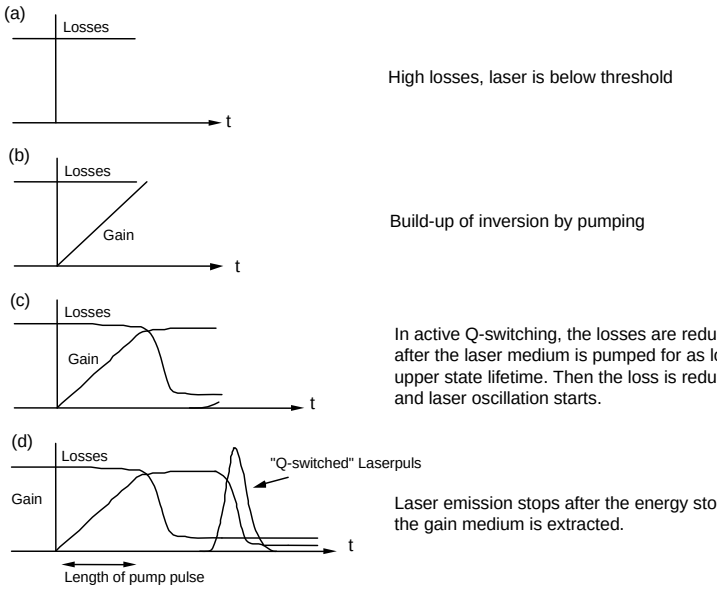

Figure 7.27: Gain and loss dynamics of an actively Q-switched laser.

Fig. 7.27 shows the principle dynamics of an actively Q-switched laser. The laser is pumped by a pump pulse with a length on the order of the upper-state lifetime, while the intracavity losses are kept high enough so that the laser can not reach threshold. At this point, the laser medium acts as energy storage with the energy slowly relaxing by spontaneous and nonradiative transitions. Intracavity loss is suddenly reduced, for example by a rotating cavity mirror. The laser is pumped way above threshold and the light field builts exponentially up until the pulse energy comes close to the saturation energy of the gain medium. The gain saturates and its energy is extracted, causing the laser to be shut off by the pulse itself.

A typical actively Q-switched pulse is asymmetric: The rise time is proportional to the net gain after the Q-value of the cavity is actively switched to a high value. The light intensity grows proportional to $2g_0/T_R$. When the gain is depleted, the fall time mostly depends on the cavity decay time τ_p, see Figure 7.28. For short Q-switched pulses a short cavity length, high gain and a large change in the cavity Q is necessary. If the Q-switch is not fast, the pulse width may be limited by the speed of the switch. Typical time scales for electro-optical and acousto-optical switches are 10 ns and 50 ns, respectively

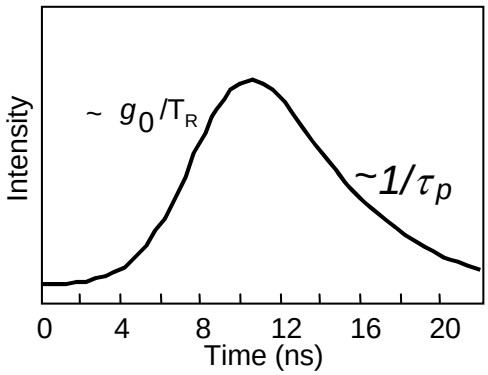

Figure 7.28: Asymmetric actively Q-switched pulse.

For example, with a diode-pumped Nd:YAG microchip laser [15] using an electro-optical switch based on $LiTaO_3$ Q-switched pulses as short as 270 ps at repetition rates of 5 kHz, peak powers of 25 kW at an average power of 34 mW, and pulse energy of 6.8 μJ have been generated (Figure 7.29).

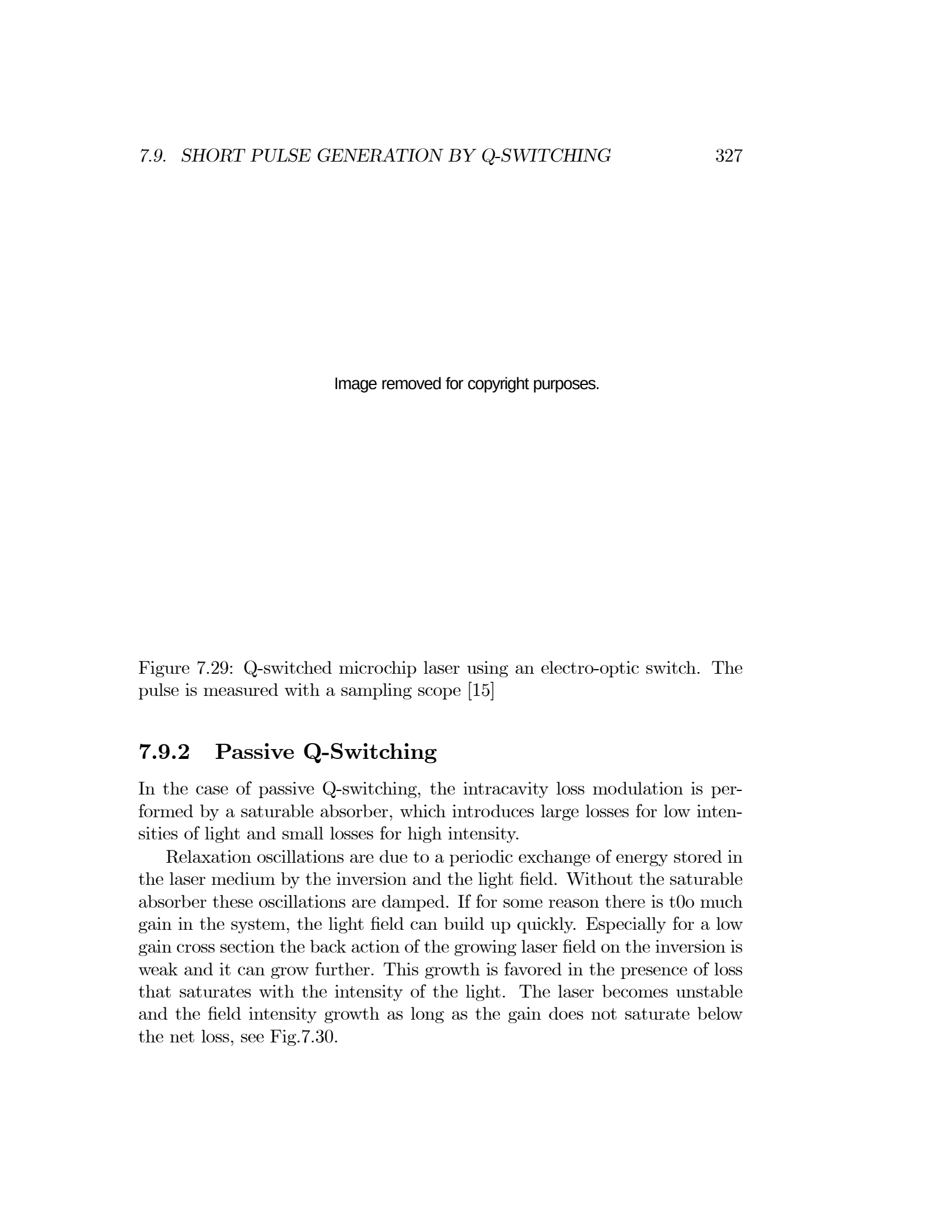

Figure 7.29: Q-switched microchip laser using an electro-optic switch. The pulse is measured with a sampling scope [15]

7.9.2 Passive Q-Switching

In the case of passive Q-switching, the intracavity loss modulation is performed by a saturable absorber, which introduces large losses for low intensities of light and small losses for high intensity.

Relaxation oscillations are due to a periodic exchange of energy stored in the laser medium by the inversion and the light field. Without the saturable absorber these oscillations are damped. If for some reason there is t0o much gain in the system, the light field can build up quickly. Especially for a low gain cross section the back action of the growing laser field on the inversion is weak and it can grow further. This growth is favored in the presence of loss that saturates with the intensity of the light. The laser becomes unstable and the field intensity growth as long as the gain does not saturate below the net loss, see Fig.7.30.

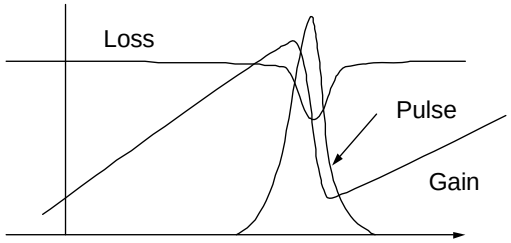

Figure 7.30: Gain and loss dynamics of a passively Q-switched laser

The saturable absorber leads to a destabilization of the relaxation oscillations resulting in the giant laser pulses.

7.10 Short pulse generation by mode locking

Q-switching is a single mode pheonomenon, i.e. the pulse build-up and decay occurs over many round-trips via build-up of energy and decay in a single (or a few) longitudinal mode. If one could get several longitudinal modes lasing in a phase coherent fashion with resepct to each other, these modes would be the Fourier components of a periodic pulse train emitted from the laser. Then a single pulse is traveling inside the laser cavity. This is called mode locking and the pulses generated are much shorter than the cavity round-trip time due to interference of the fields from many modes. The electric field can be written as a superpostion of the longitudinal modes. We neglect polarization for the moment.

$$E(z,t) = \Re\left[\sum_m \hat{E}_m e^{\mathrm{j}(\omega_m t - k_m z + \phi_m)}\right], \tag{7.60a}$$

$$\omega_m = \omega_0 + m\Delta\omega = \omega_0 + \frac{m\pi c}{\ell}, \tag{7.60b}$$

$$k_m = \frac{\omega_m}{c}. \tag{7.60c}$$

Equation (7.60a) can be rewritten as

$$E(z,t) = \Re\left\{ e^{\mathrm{j}\omega_0(t-z/c)} \sum_m \hat{E}_m e^{\mathrm{j}(m\Delta\omega(t-z/c)+\phi_m)} \right\} \tag{7.61a}$$

$$= \Re\left[A(t-z/c) e^{\mathrm{j}\omega_0(t-z/c)} \right] \tag{7.61b}$$

with the complex envelope

$$A\left(t-\frac{z}{c}\right) = \sum_m E_m e^{\mathrm{j}(m\Delta\omega(t-z/c)+\phi_m)} = \text{complex envelope (slowly varying).} \tag{7.62}$$

$e^{\mathrm{j}\omega_0(t-z/c)}$ is the carrier wave (fast oscillation). Here, both the carrier and the envelope travel with the same speed (no dispersion assumed). The envelope function is periodic with period

$$T = \frac{2\pi}{\Delta\omega} = \frac{2\ell}{c} = \frac{L}{c}, \tag{7.63}$$

where L is the optical round-trip length in the cavity. If we assume that N modes with equal amplitudes $E_m = E_0$ and equal phases $\phi_m = 0$ are lasing, the envelope is given by

$$A(z,t) = E_0 \sum_{m=-(N-1)/2}^{(N-1)/2} e^{\mathrm{j}(m\Delta\omega(t-z/c))}. \tag{7.64}$$

With

$$\sum_{m=0}^{q-1} a^m = \frac{1-a^q}{1-a}, \tag{7.65}$$

we obtain

$$A(z,t) = E_0 \frac{\sin\left[\frac{N\Delta\omega}{2}\left(t-\frac{z}{c}\right)\right]}{\sin\left[\frac{\Delta\omega}{2}\left(t-\frac{z}{c}\right)\right]}. \tag{7.66}$$

The laser intensity I is proportional to $E(z,t)^2$ averaged over one optical cycle: $I \sim |A(z,t)|^2$. At $z = 0$, we obtain

$$I(t) \sim |E_0|^2 \frac{\sin^2\left(\frac{N\Delta\omega t}{2}\right)}{\sin^2\left(\frac{\Delta\omega t}{2}\right)}. \tag{7.67}$$

The periodic pulses given by Eq. (7.67) have

- the period: $T = 1/\Delta f = L/c$
- pulse duration: $\Delta t = \frac{2\pi}{N\Delta\omega} = \frac{1}{N\Delta f}$
- peak intensity $\sim N^2|E_0|^2$
  - average intensity $\sim N|E_0|^2 \Rightarrow$ peak intensity is enhanced by a factor N.

If the phases of the modes are not locked, i.e. ϕ_m is a random sequence then the intensity fluctuates randomly about its average value ($\sim N|E_0|^2$), which is the same as in the mode-locked case. Figure 7.31 shows the intensity of a modelocked laser versus time,if the relative phases of the modes to each other is (a) constant and (b) random

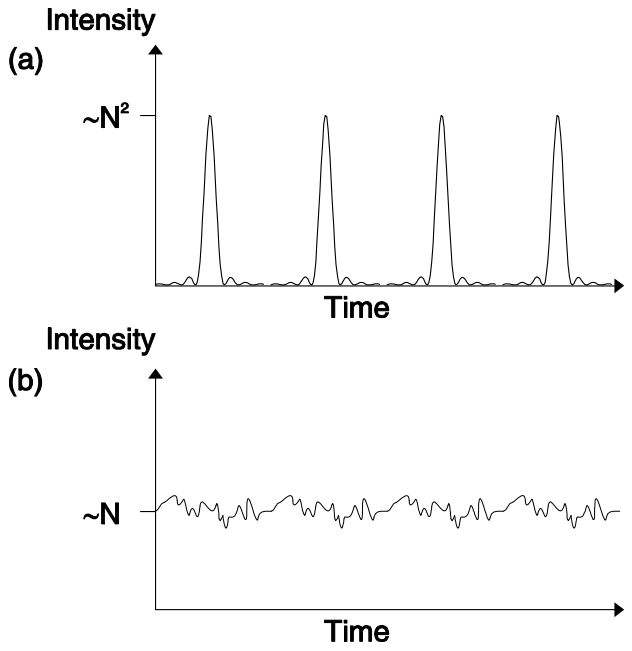

Figure 7.31: Laser intensity versus time from a mode-locked laser with (a) perfectly locked phases and (b) random phases.

We are distinguishing between active modelocking, where an external loss modulator is inserted in the cavity to generate modelocked pulses, and passive modelocking, where the pulse is modulating the intracavity itself via a saturable absorber.

7.10.1 Active Mode Locking

Active mode locking was first investigated in 1970 by Kuizenga and Siegman [16] and later by Haus [17] . In the approach by Haus, modelocking is treated as a pulse propagation problem.

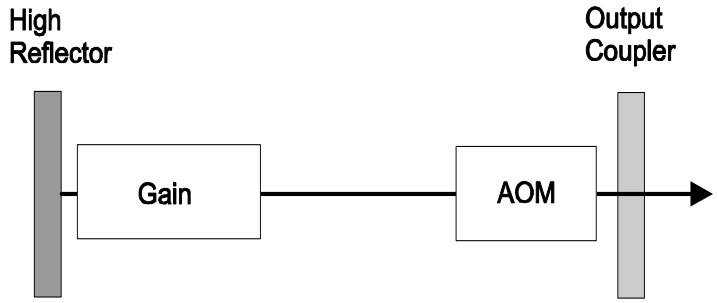

Figure 7.32: Actively modelocked laser with an amplitude modulator (Acousto-Optic-Modulator).

The pulse is shaped in the resonator by the finite bandwidth of the gain and the loss modulator, which periodically varies the intracavity loss according to $q(t) = M\left(1 - \cos(\omega_M t)\right)$. The modulation frequency has to be precisely tuned to the resonator round-trip time, $\omega_M = 2\pi/T_R$, see Fig.7.32. The mode locking process is then described by the master equation for the slowly varying pulse envelope

$$T_R \frac{\partial A}{\partial T} = \left[g(T) + D_g \frac{\partial^2}{\partial t^2} - l - M\left(1 - \cos(\omega_M t)\right) \right] A. \tag{7.68}$$

This equation can be interpreted as the total pulse shaping due to gain, loss and modulator within one roundtrip, see Fig.7.33.

If we fix the gain in Eq. (7.68) at its stationary value, what ever it might be, Eq.(7.68) is a linear p.d.e, which can be solved by separation of variables. The pulses, we expect, will have a width much shorter than the round-trip time T_R. They will be located in the minimum of the loss modulation where the cosine-function can be approximated by a parabola and we obtain

$$T_R \frac{\partial A}{\partial T} = \left[g - l + D_g \frac{\partial^2}{\partial t^2} - M_s t^2 \right] A. \tag{7.69}$$

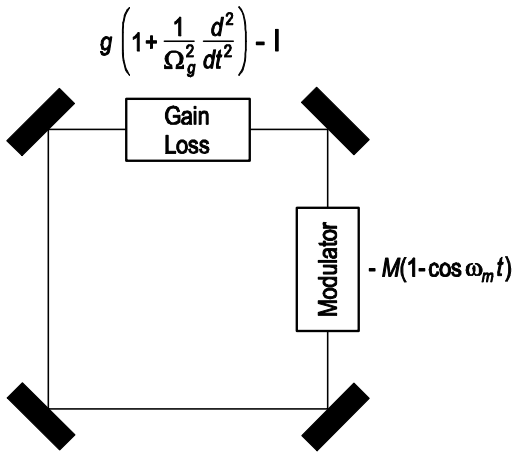

Figure 7.33: Schematic representation of the master equation for an actively mode-locked laser.

M_s is the modulation strength, and corresponds to the curvature of the loss modulation in the time domain at the minimum loss point

$$D_g = \frac{g}{\Omega_g^2}, \tag{7.70}$$

$$M_s = \frac{M\omega_M^2}{2}. \tag{7.71}$$

The differential operator on the right side of (7.69) corresponds to the Schrödinger-Operator of the harmonic oscillator problem. Therefore, the eigen functions of this operator are the Hermite-Gaussians

$$A_n(T,t) = A_n(t)e^{\lambda_n T/T_R}, \tag{7.72}$$

$$A_n(t) = \sqrt{\frac{W_n}{2^n\sqrt{\pi}n!\tau_a}}H_n(t/\tau_a)e^{-\frac{t^2}{2\tau_a^2}}, \tag{7.73}$$

where τ_a determines the pulse width of the Gaussian pulse. The width is given by the fourth root of the ratio between gain dispersion and modulator strength

$$\tau_a = \sqrt[4]{D_g/M_s}. \tag{7.74}$$

Note, from Eq. (7.72) we see that the gain per round-trip of each eigenmode

is given by λ_n (or in general the real part of λ_n), which is given by

$$\lambda_n = g_n - l - 2M_s\tau_a^2(n + \frac{1}{2}). \tag{7.75}$$

The corresponding saturated gain for each eigen solution is given by

$$g_n = \frac{1}{1 + \frac{W_n}{P_L T_R}}, \tag{7.76}$$

where W_n is the energy of the corresponding solution and $P_L = E_L/\tau_L$ the saturation power of the gain. Eq. (7.75) shows that for a given g the eigen solution with $n = 0$, the ground mode, has the largest gain per roundtrip. Thus, if there is initially a field distribution which is a superpostion of all eigen solutions, the ground mode will grow fastest and will saturate the gain to a value

$$g_s = l + M_s\tau_a^2. \tag{7.77}$$

such that $\lambda_0 = 0$ and consequently all other modes will decay since $\lambda_n < 0$ for $n \geq 1$. This also proves the stability of the ground mode solution [17]. Thus active modelocking without detuning between resonator round-trip time and modulator period leads to Gaussian steady state pulses with a FWHM pulse width

$$\Delta t_{FWHM} = 2\ln 2\tau_a = 1.66\tau_a. \tag{7.78}$$

The spectrum of the Gaussian pulse is given by

$$\tilde{A}_0(\omega) = \int_{-\infty}^{\infty} A_0(t)e^{i\omega t}dt \tag{7.79}$$

$$= \sqrt{\sqrt{\pi}W_n\tau_a}e^{-\frac{(\omega\tau_a)^2}{2}}, \tag{7.80}$$

and its FWHM is

$$\Delta f_{FWHM} = \frac{1.66}{2\pi\tau_a}. \tag{7.81}$$

Therfore, the time-bandwidth product of the Gaussian is

$$\Delta t_{FWHM} \cdot \Delta f_{FWHM} = 0.44. \tag{7.82}$$

The stationary pulse shape of the modelocked laser is due to the parabolic loss modulation (pulse shortening) in the time domain and the parabolic filtering (pulse stretching) due to the gain in the frequency domain, see Figs.

7.34 and 7.35. The stationary pulse is achieved when both effects balance. Since external modulation is limited to electronic speed and the pulse width does only scale with the inverse square root of the gain bandwidth actively modelocking typically only results in pulse width in the range of 10-100ps.

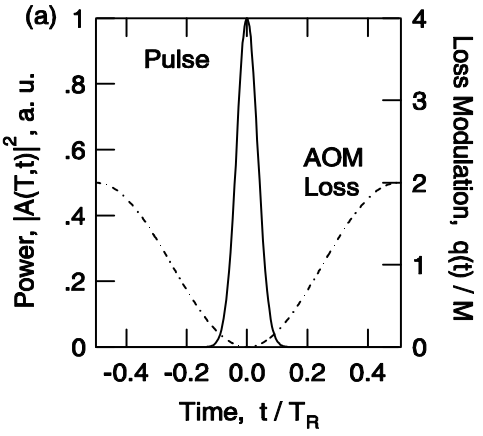

Figure 7.34: Loss modulation leads to pulse shortening in each roundtrip

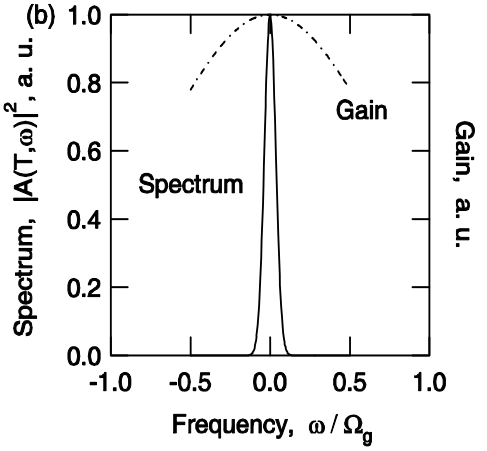

Figure 7.35: The finite gain bandwidth broadens the pulse in each roundtrip. For a certain pulse width there is balance between the two processes.

For example: Nd:YAG; $2l = 2g = 10\%$, $\Omega_g = \pi\Delta f_{FWHM} = 0.65$ THz,

$M = 0.2$, $f_m = 100$ MHz, $D_g = 0.24$ ps^2, $M_s = 4 \cdot 10^{16} s^{-1}$, $\tau_p \approx 99$ ps.

With the pulse width (7.74), Eq.(7.77) can be rewritten in several ways

$$g_s = l + M_s \tau_a^2 = l + \frac{D_g}{\tau_a^2} = l + \frac{1}{2} M_s \tau_a^2 + \frac{1}{2} \frac{D_g}{\tau_a^2}, \tag{7.83}$$

which means that in steady state the saturated gain is lifted above the loss level l, so that many modes in the laser are maintained above threshold. There is additional gain necessary to overcome the loss of the modulator due to the finite temporal width of the pulse and the gain filter due to the finite bandwidth of the pulse. Usually

$$\frac{g_s - l}{l} = \frac{M_s \tau_a^2}{l} \ll 1, \tag{7.84}$$

since the pulses are much shorter than the round-trip time. The stationary pulse energy can therefore be computed from

$$g_s = \frac{1}{1 + \frac{W_s}{P_L T_R}} = l. \tag{7.85}$$

The name modelocking originates from studying this pulse formation process in the frequency domain. Note, the term

$$-M \left[1 - \cos(\omega_M t)\right] A$$

generates sidebands on each cavity mode present according to

$$\begin{aligned} & -M \left[1 - \cos(\omega_M t)\right] \exp(j\omega_{n_0} t) \\ = \; & -M \left[\exp(j\omega_{n_0} t) - \frac{1}{2} \exp(j(\omega_{n_0} t - \omega_M t)) - \frac{1}{2} \exp(j(\omega_{n_0} t + \omega_M t))\right] \\ = \; & M \left[-\exp(j\omega_{n_0} t) + \frac{1}{2} \exp(j\omega_{n_0 - 1} t) + \frac{1}{2} \exp(j\omega_{n_0 + 1} t)\right] \end{aligned}$$

if the modulation frequency is the same as the cavity round-trip frequency. The sidebands generated from each running mode is injected into the neighboring modes which leads to synchronisation and locking of neighboring modes, i.e. mode-locking, see Fig.7.36

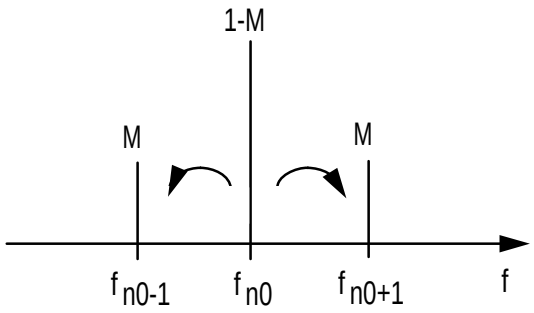

Figure 7.36: Modelocking in the frequency domain: The modulator transvers energy from each mode to its neighboring mode, thereby redistributing energy from the center to the wings of the spectrum. This process seeds and injection locks neighboring modes.

7.10.2 Passive Mode Locking

Electronic loss modulation is limited to electronic speeds. Therefore, the curvature of the loss modulation that determines the pulse length is limited. It is desirable that the pulse itself modulates the loss. The shorter the pulse the sharper the loss modulation and eventually much shorter pulses can be reached.

The dynamics of a laser modelocked with a fast saturable absorber can also be easily understood using the master equation (7.68) and replacing the loss due to the modulator with the loss from a saturable absorber. For a fast saturable absorber, the losses q react instantaneously on the intensity or power $P(t) = |A(t)|^2$ of the field

$$q(A) = \frac{q_0}{1 + \frac{|A|^2}{P_A}}, \tag{7.86}$$

where P_A is the saturation power of the absorber. Such absorbers can be made out of semiconductor materials or nonlinear optical effects can be used to create artificial saturable absorption, such as in Kerr lens mode locking.

There is no analytic solution of the master equation (7.68) when the loss modulation is replaced by the absorber response (7.86). We can however make expansions on the absorber response to get analytic insight. If the absorber is not saturated, we can expand the response (7.86) for small

intensities

$$q(A) = q_0 - \gamma|A|^2, \tag{7.87}$$

with the saturable absorber modulation coefficient $\gamma = q_0/P_A$. The constant nonsaturated loss q_0 can be absorbed in the losses $l_0 = l + q_0$. The resulting master equation is

$$T_R \frac{\partial A(T,t)}{\partial T} = \left[g - l_0 + D_f \frac{\partial^2}{\partial t^2} + \gamma|A|^2 \right] A(T,t). \tag{7.88}$$

Up to the imaginary unit, this equation is similar to a type of nonlinear Schroedinger Equation, i.e. the potential depends on the wave function itself. One finds as a possible stationary solution

$$A_s(T,t) = A_s(t) = A_0 \text{sech}\left(\frac{t}{\tau}\right). \tag{7.89}$$

Note, there is

$$\frac{d}{dx}\text{sech}x = -\tanh x \, \text{sech}x, \tag{7.90}$$

$$\begin{aligned} \frac{d^2}{dx^2}\text{sech}x &= \tanh^2 x \, \text{sech}x - \text{sech}^3 x, \\ &= \left(\text{sech}x - 2\,\text{sech}^3 x\right). \end{aligned} \tag{7.91}$$

Substitution of the solution (7.89) into the master equation (7.88), and assuming steady state, results in

$$\begin{aligned} 0 = &\left[(g - l_0) + \frac{D_f}{\tau^2}\left[1 - 2\text{sech}^2\left(\frac{t}{\tau}\right)\right]\right. \\ &\left. + \gamma|A_0|^2 \text{sech}^2\left(\frac{t}{\tau}\right)\right] \cdot A_0 \text{sech}\left(\frac{t}{\tau}\right). \end{aligned} \tag{7.92}$$

Comparison of the coefficients with the sech- and sech^3-expressions leads to a condition for the peak pulse intensity and pulse width, τ, and for the saturated gain

$$\frac{D_f}{\tau^2} = \frac{1}{2}\gamma|A_0|^2, \tag{7.93}$$

$$g = l_0 - \frac{D_f}{\tau^2}. \tag{7.94}$$

From Eq.(7.93) and with the pulse energy of a sech pulse

$$W = \int_{-\infty}^{+\infty} 2|A_s(t)|^2 dt = 2|A_0|^2\tau, \tag{7.95}$$

follows

$$\tau = \frac{4D_f}{\gamma W}. \tag{7.96}$$

$$g_s(W) = \frac{g_0}{1 + \frac{W}{P_L T_R}} \tag{7.97}$$

Equation (7.94) together with (7.96) determines the pulse energy

$$\begin{aligned} g_s(W) &= \frac{g_0}{1 + \frac{W}{P_L T_R}} = l_0 - \frac{D_f}{\tau^2} \\ &= l_0 - \frac{(\gamma W)^2}{16 D_g} \end{aligned} \tag{7.98}$$

Figure 7.37 shows the time dependent variation of gain and loss in a laser modelocked with a fast saturable absorber on a normalized time scale.

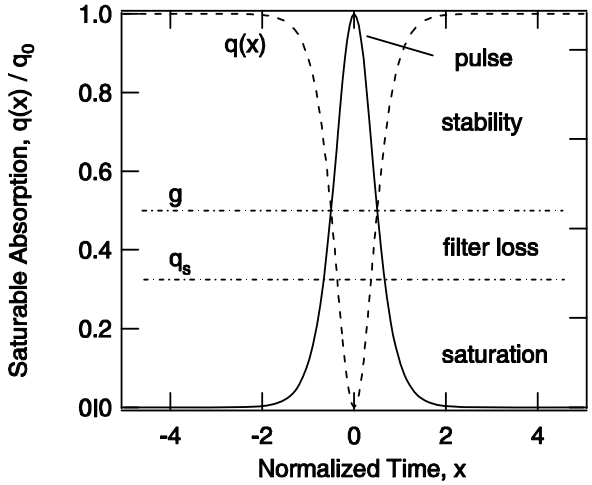

Figure 7.37: Gain and loss in a passively modelocked laser using a fast saturable absorber on a normalized time scale $x = t/\tau$. The absorber is assumed to saturate linearly with intensity according to $q(A) = q_0\left(1 - \frac{|A|^2}{A_0^2}\right)$.

Here, we assumed that the absorber saturates linearly with intensity up to a maximum value $q_0 = \gamma A_0^2$. If this maximum saturable absorption is completely exploited, see Figure 7.38.

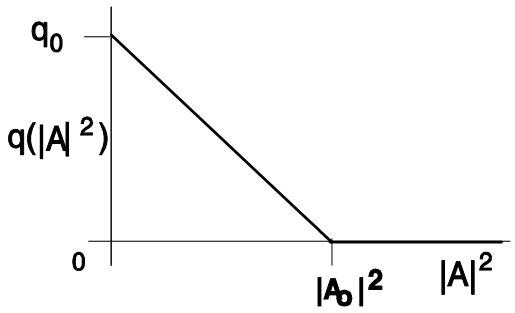

Figure 7.38: Saturation characteristic of an ideal saturable absorber

The minimum pulse width achievable with a given saturable absorption q_0 results from Eq.(7.93)

$$\frac{D_f}{\tau^2} = \frac{q_0}{2}, \tag{7.99}$$

to be

$$\tau = \sqrt{\frac{2}{q_0}} \frac{1}{\Omega_f}. \tag{7.100}$$

Note that in contrast to active modelocking the achievable pulse width is now scaling with the inverse gain bandwidth. This gives much shorter pulses. Figure 7.37 can be interpreted as follows: In steady state, the saturated gain is below loss, by about one half of the exploited saturable loss before and after the pulse. This means that there is net loss outside the pulse, which keeps the pulse stable against growth of instabilities at the leading and trailing edge of the pulse. If there is stable mode-locked operation, there must always be net loss far away from the pulse, otherwise, a continuous wave signal running at the peak of the gain would experience more gain than the pulse and would break through. From Eq.(7.93) it follows, that one third of the exploited saturable loss is used up during saturation of the aborber and actually only one sixth is used to overcome the filter losses due to the finite gain bandwidth. Note, there is a limit to the mimium pulse width. This limit is due to the saturated gain (7.94), $g_s = l + \frac{1}{2}q_0$. Therefore, from

Eq.(7.100), if we assume that the finite bandwidth of the laser is set by the gain, i.e. $D_f = D_g = \frac{g}{\Omega_g^2}$, we obtain for $q_0 \gg l$

$$\tau_{\min} = \frac{1}{\Omega_g} \tag{7.101}$$

for the linearly saturating absorber model. This corresponds to mode locking over the full bandwidth of the gain medium, as for a sech-shaped pulse, the time-bandwidth product is 0.315, and therefore,

$$\Delta f_{FWHM} = \frac{0.315}{1.76 \cdot \tau_{\min}} = \frac{\Omega_g}{1.76 \cdot \pi}. \tag{7.102}$$

As an example, for the Ti:sapphire laser this corresponds to $\Omega_g = 240$ THz, $\tau_{\min} = 3.7$ fs, $\tau_{FWHM} = 6.5$ fs, which is in good agreement with experimentally observed results [19].

This concludes the introdcution into ultrashort pulse generation by mode locking.

Bibliography

[1] R. W. Hellwarth, Eds., Advances in Quantum Electronics, Columbia Press, New York (1961).

[2] A. E. Siegman, "Lasers," University Science Books, Mill Valley, California (1986).

[3] O. Svelto, "Principles of Lasers," Plenum Press, NY 1998.

[4] http://www.llnl.gov/nif/library/aboutlasers/how.html

[5] T. H. Maimann, "Stimulated optical radiation in ruby", Nature **187**, 493-494, (1960).

[6] B.E.A. Saleh and M.C. Teich, "Fundamentals of Photonics," John Wiley and Sons, Inc., 1991.

[7] M. J. Weber, "Handbook of Lasers", CRC Press, 2000.

[8] A. Javan, W. R. Bennett and D. H. Herriott, "Population Inversion and Continuous Optical Maser Oscillation in a Gas Discharge Containing a He-Ne Mixture," Phys. Rev. Lett. **6,** (1961).

[9] W. R. Bennett, Applied Optics, Supplement 1, Optical Masers, 24, (1962).

[10] W. Koechner, "Solid-State Lasers," Springer Verlag (1990).

[11] R F Kazarinov and R A Suris, "Amplification of electromagnetic waves in a semiconductor superlattice," Sov. Phys. Semicond. **5**, p. 707 (1971).

[12] J. Faist, F. Capasso, D. L. Sivco, C. Sirtori, A. L. Hutchinson, A. Y. Cho, "Quantum cascade laser," Science **264**, p. 553 (1994).

[13] B. S. Williams, H. Callebaut, S. Kumar, Q. Hu and J. L. Reno, "3.4-THz quantum cascade laser based on longitudinal-optical-phonon scattering for depopulation," Appl. Phys. Lett. **82**, p. 1015-1017 (2003).

[14] D. Kopf, F. X. Kärtner, K. J. Weingarten, M. Kamp, and U. Keller, "Diode-pumped mode-locked Nd:glass lasers with an antiresonant Fabry-Perot saturable absorber," Optics Letters **20**, p. 1169 (1995).

[15] J. J. Zayhowski, C. Dill, "Diode-pumped passively Q-switched picosecond microchip lasers," Opt. Lett. **19**, pp. 1427 – 1429 (1994).

[16] D. J. Kuizenga and A. E. Siegman, "FM and AM modelocking of the homogeneous laser - part I: theory," IEEE J. Qunat. Electron. **6**, pp. 694 – 701 (1970).

[17] H. A. Haus, "A Theory of Forced Mode Locking", IEEE Journal of Quantum Electronics **QE-11**, pp. 323 - 330 (1975).

[18] H. A. Haus, "Theory of modelocking with a fast saturable absorber," J. Appl. Phys. **46**, pp. 3049 – 3058 (1975).

[19] R. Ell, U. Morgner, F.X. Kärtner, J.G. Fujimoto, E.P. Ippen, V. Scheuer, G. Angelow, T. Tschudi: Generation of 5-fs pulses and octave-spanning spectra directly from a Ti:Sappire laser, Opt. Lett. **26**, 373-375 (2001)